

# Comparative Study Between Measurement and Predictions Using Geometrical Optics and Uniform Theory of Diffraction for Case of Non-Line-of-Sight (NLOS) in Indoor Environment

E. M. Cheng · Zulkifly Abbas · M. Fareq · K. Y. Lee ·  
K. Y. You · S. F. Khor

Published online: 19 November 2012  
© Springer Science+Business Media New York 2012

**Abstract** This paper describes the investigation and comparison of the accuracy of a deterministic model for a WLAN system in the indoor environment. The measurement system consisted of a spectrum analyzer and a log-periodic antenna. Non-line-of-sight (NLOS) propagation (in furnished rooms) was investigated. All the measurement sites mentioned in this paper are located in the Division of Information Technology at Universiti Putra Malaysia. The furnished rooms mentioned above were a teaching laboratory and a computer laboratory. The measured path losses were compared with the results obtained using deterministic models, namely the geometrical optics model and the uniform theory of diffraction model with the aid of image theory. The predicted results showed good agreement with the measured

---

E. M. Cheng (✉)

School of Mechatronic Engineering, Universiti Malaysia Perlis (UniMAP), 02600 Arau, Perlis, Malaysia  
e-mail: emcheng@unimap.edu.my

Z. Abbas

Department of Physics, Faculty of Science, Universiti Putra Malaysia (UPM),  
43400 Serdang, Malaysia  
e-mail: za@fsas.upm.edu.my

M. Fareq · S. F. Khor

School of Electrical Systems Engineering, Universiti Malaysia Perlis (UniMAP),  
02000 Arau, Perlis, Malaysia  
e-mail: mfareq@unimap.edu.my

S. F. Khor

e-mail: sfkhor@unimap.edu.my

K. Y. Lee

Department of Electrical and Electronic Engineering, Faculty of Engineering and Science,  
Universiti Tunku Abdul Rahman (UTAR), 46200 Petaling Jaya, Selangor, Malaysia  
e-mail: kylee@utar.edu.my

K. Y. You

Department of Radio Communication Engineering, Faculty of Electrical Engineering,  
Universiti Teknologi Malaysia (UTM), 81310 Skudai, Malaysia  
e-mail: kyyou@fke.utm.my

data for the NLOS environment, with an absolute mean error that ranged between 1.61 and 3.07 dB.

**Keywords** Geometrical optics · Uniform theory of diffraction · Diffraction

## 1 Introduction

As we entered the twenty-first century twelve years ago, Information Technology (IT) and communications were leading a revolution that changed the way we live. The numbers of cellular telephone subscribers, the numbers of people accessing the Internet, the growth of electronic businesses, and the abundance of companies on the Web have led to the rapid development of personal communication systems (PCSs) and wireless LAN systems in recent years. As a result, there is an increasing need for an efficient way to evaluate the propagation of radio waves in buildings. In addition, it is also very important to determine the ideal location of the access point in order to enhance system performance. Therefore, the need to predict the propagation of radio waves in the indoor environment has formed the basis for optimizing the location of the access point, hence it has become an important research topic. Access to information has become a necessity, and the information that is available on the Internet and the ease with which it can be accessed and used have provided tools that would have been unavailable without this communication facility but that have become indispensable to today's professionals and others. As a result, the Internet has become an indispensable tool as well as an open window for people to showcase their information to the world.

Theoretically, in order to make sure that the quality of wireless access to the Internet is maintained, wireless service providers had to characterize the propagation medium by conducting measurements of the propagation of radio waves every building in which they deployed their WLAN systems. As a result, the installation cost was very high due to the labor costs and the high cost of the equipment involved. Therefore, it is necessary to develop a model to predict the propagation characteristics of the indoor environment. Once a propagation model has been verified based on the parameters or information of the given environment, the model is developed to provide a propagation characteristic for initial evaluation. After that, quick measurements would have to be conducted at positions where the signal is poor. This approach is much more practical in practice, and, in addition, the cost of installation is much lower than the one discussed formerly, decreasing the cost of implementation for the organization.

Actually, the propagation of radio waves indoors is not influenced by weather conditions, such as rain, snow, or clouds, as is outdoor propagation, but it can be affected by the layout of the building, especially the use of some specific building materials [1]. Owing to the characteristics of reflection, refraction, and diffraction of radio waves by obstacles inside the building, such as walls, windows, doors, and furniture, the transmitted signal often reaches the receiver through more than one path, resulting in a phenomenon known as multipath fading.

## 2 Measurement Setup

### 2.1 Measurement Equipment

The measurement of electric field strength is conducted using an ADVANTEST U3641 spectrum analyzer and an AHS/SAS-519-4 log periodic antenna. This antenna has one

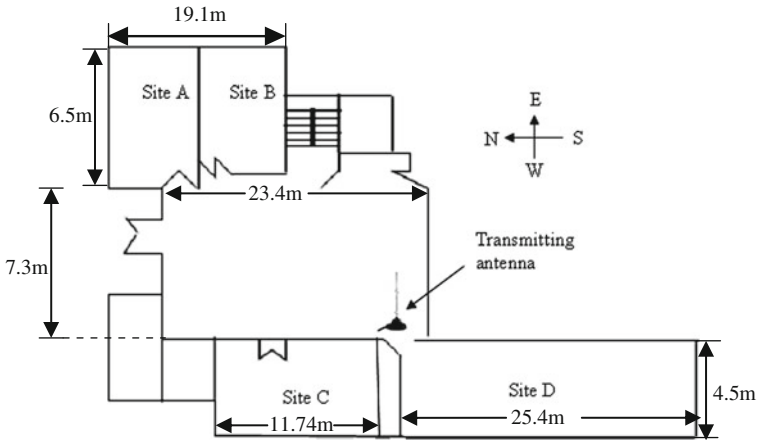


**Fig. 1** Measurement sites

directional radiation pattern (Half power beamwidth, typical angle  $60^\circ \times 80^\circ$ ). The gain for the AHS/SAS-519-4 log periodic antenna is 6.7 dBi. For low frequency signal ( $<2$  GHz), the effect of side lobes for log periodic antenna is relatively small compare to the main lobe (main half beamwidth).

Meanwhile, the transmitting antenna used is 5 dBi Magnetic Mount Omni Antenna which the compatible frequency range is from 2,400 to 2,500 MHz. However, the bandwidth of operating frequency that can be detected by spectrum analyzer is ranging from 2.403 to 2.422 GHz, which is approximately 2.4 GHz.

## 2.2 Measurement Environment

The Division Information Technology Center is the operating center from which the entire Internet network in UPM is operated. The Division Information Technology Center was chosen as the site for taking measurements in this project because the WLAN service was provided inside the building that houses Division Information Technology Center. Blueprint of the measurement site can be referred to Fig. 1. The measurement was conducted at Site A (Fig. 2), Site B (Fig. 3), Site C (Fig. 4), and Site D (Fig. 5). The antenna was mounted on the ceiling at location shown in Fig. 1 at a height of 2.58 m above the floor. There were five or six measurement positions at every measurement site (Site A–D).

There were more than 20 computers along with the associated furniture provided in Site A, Site B, and Site C. Each site that mentioned formerly, were equipped with more than 20 units of computers in furnished computer laboratories. Two concrete pillars were located at the center of each of the three sites. These were the main reason for the decrease in the strength of the signal. A glass wall divided Site A, Site B, and Site C, separating some of each site from the area where the transmitter was located. Meanwhile, each measuring position in Site D is blocked by a wooden door and it was the measurement site which was closest to the transmitting antenna. Five measuring position were chosen in each of Sites A, B, C and D.

Site D was the Network Operating Room, and five measuring positions also were chosen in this Site. There were two concrete pillars in the center of Site D, similar to Sites A, B, and C. Computers and associated furniture (desks and chairs) were also located there. Unlike Sites A, B, and C, there was a hard partition in Site D.



**Fig. 2** Site A



**Fig. 3** Site B

Also, five positions were chosen as measuring sites. It is found that the signal could not be detected by the spectrum analyzer in the interior of the server room. The farthest region from the transmitter is the shadow region in the Network Operating Room where the coverage signal is not reachable in this region. The interior corridor (Fig. 6) is like a tunnel. The direct ray (or direct transmitted) from the source was assumed to be absent in that region, but a weak and negligible signal existed in the interior region due to multiple reflections of scattered rays [2].



**Fig. 4** Site C

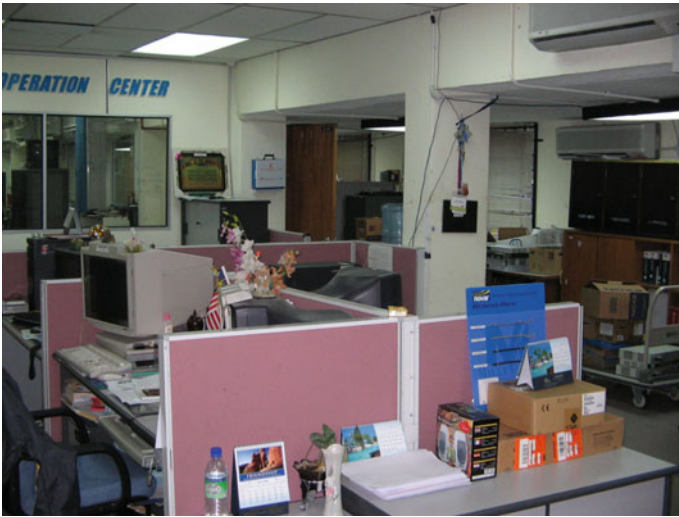


**Fig. 5** Site D

### 3 GO and UTD Field Prediction

#### 3.1 Geometrical Optics (GO)

Geometrical optics is a high-frequency method for approximating wave propagation for incident, reflected, and refracted fields. It uses the ray concept, so it is often referred to as ray optics. It was developed to analyze the propagation of light (waves) at high frequencies [3].



Fig. 6 Inner part of Site D

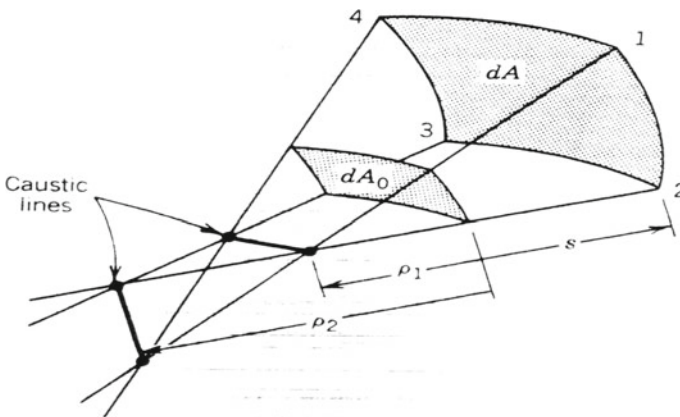


Fig. 7 Astigmatic tube of rays [3]

The final form of the GO equation is:

$$E(s) = E_0(0)e^{j\varphi_0(0)} \sqrt{\frac{\rho_1 \rho_2}{(\rho_1 + s)(\rho_2 + s)}} e^{-j\beta s}, \tag{1}$$

where  $\varphi_0(0)$  = field phase at reference point ( $s = 0$ ), and the parameters  $\rho_1$ ,  $\rho_2$ , and  $s$  are as illustrated in Fig. 7. The spreading factor,  $\sqrt{\frac{\rho_1 \rho_2}{(\rho_1 + s)(\rho_2 + s)}}$ , can be reduced to  $\sqrt{\frac{1}{s}}$ , as expressed in [4].

The GO field is a very useful description of the incident field, reflected field, and refracted field. However, such a description leads to incorrect predictions when considering fields in the shadow region behind an obstruction, since it predicts that no fields exist in the shadow region. This suggested that there is an infinitely sharp transition from the shadow region to

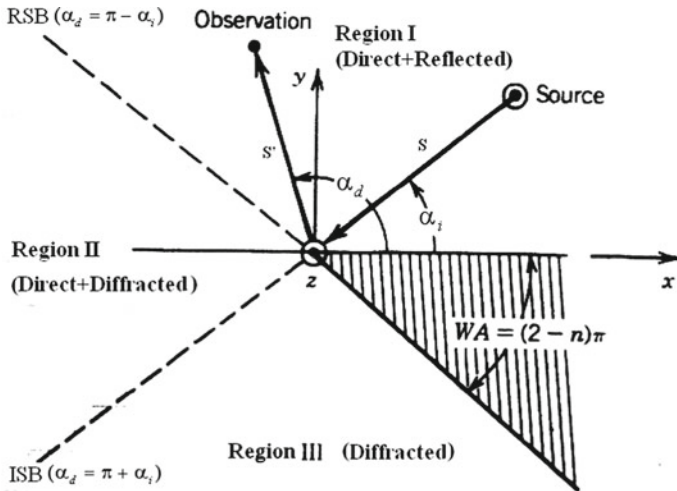


Fig. 8 Diffraction on a straight edge (top view) [3]

the illuminated region. In practice, the transition from the illuminated region to the shadow region is never completely sharp, because some energy propagates into the shadow region.

### 3.2 Uniform Theory of Diffraction (UTD)

The uniform theory of diffraction (UTD) developed by Kouyoumjian was divergent from Keller’s Geometrical Theory of Diffraction theory, and it overcame the GO’s defects in the shadow region and GTD’s defects in the vicinity of shadow boundaries. The uniform diffraction coefficient in vertical polarization is defined as [5]:

$$\begin{aligned}
 D^{\parallel} = & \frac{-e^{-j\pi/4}}{2n\sqrt{2\pi k} \sin \beta_o} \left\{ \cot \left[ \frac{\pi + (\alpha_d - \alpha_i)}{2n} \right] F[kLa^+] \right. \\
 & \times (\alpha_d - \alpha_i) + \cot \left[ \frac{\pi - (\alpha_d - \alpha_i)}{2n} \right] F[kLa^-] \\
 & \times (\alpha_d - \alpha_i) + R_o^{\parallel} \cot \left[ \frac{\pi - (\alpha_d + \alpha_i)}{2n} \right] \\
 & \left. \times F[kLa^-(\alpha_d + \alpha_i)] + \frac{R_n^{\parallel} \cot \left[ \frac{\pi + (\alpha_d + \alpha_i)}{2n} \right]}{F[kLa^+(\alpha_d + \alpha_i)]} \right\}
 \end{aligned}
 \tag{2}$$

where  $F(x) = 2j\sqrt{x}e^{jx} \int_{\sqrt{x}}^{\infty} e^{-j\tau^2} d\tau$  is a Fresnel integral,  $a^{\pm}(\alpha_d \pm \alpha_i) = 2 \cos^2 \left[ \frac{2n\pi N^{\pm} - (\alpha_d \pm \alpha_i)}{2} \right]$ ,  $N^{\pm}$  is an integer that approximately satisfies the equation  $2n\pi N^{\pm} - (\alpha_d \pm \alpha_i) = \pm \pi$ ,  $L$  is known as the displacement parameter given by  $L = \frac{s \cdot s'}{s + s'} \sin^2 \beta_0$ ,  $s$  and  $s'$  are the distances from the source field to the diffraction point on the edge and the distance from the diffraction point to the field point, respectively.  $R_o^{\parallel}$  and  $R_n^{\parallel}$  are the reflection coefficients in the vertical polarization related plane 0 with an incident angle  $\alpha_i$  and a plane  $n$  with a reflection angle  $n\pi - \alpha_d$ , respectively. The situation described by Eq. (2) is illustrated in Figs. 8 and 9.

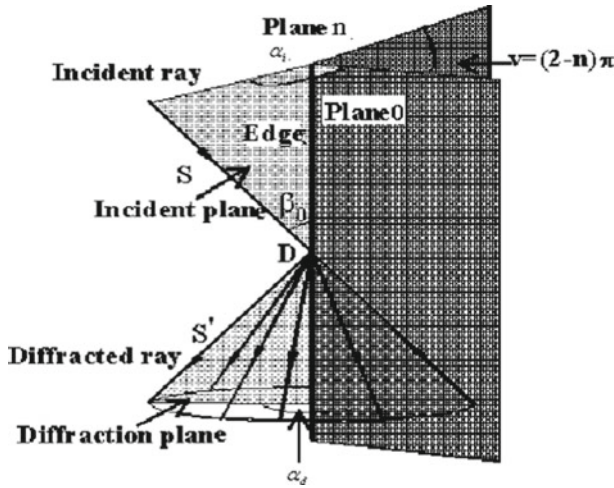


Fig. 9 Diffraction on a straight edge (elevation view) [3]

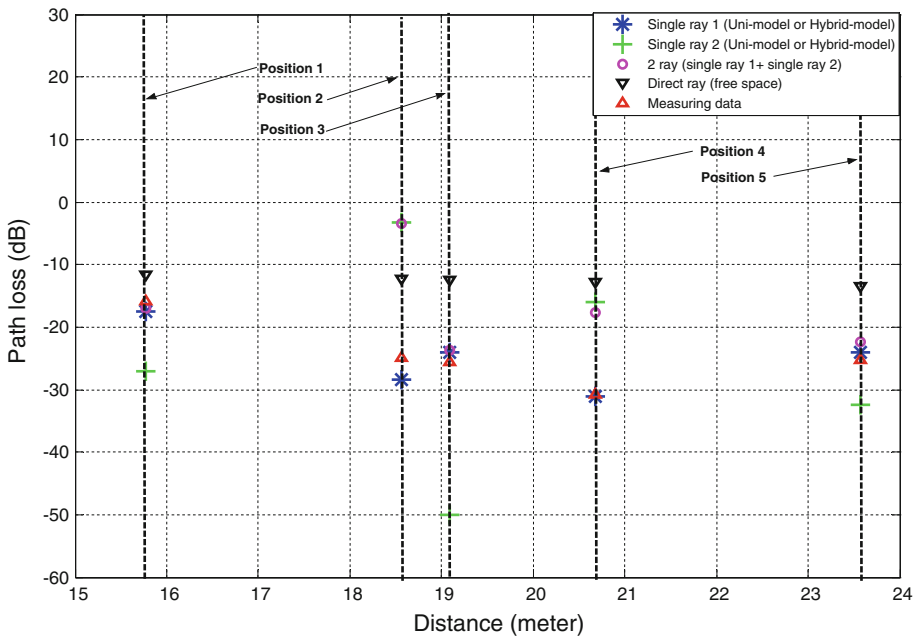


Fig. 10 Normalized path loss on Site A

### 3.3 Determination of Path Loss

Path loss can be determined by subtracting the signal strength at a specific position [Eq. 1] from the reference signal strength. The reference distance (1 m) is utilized to normalize the path loss that occurs at 1 m from the antenna so that only propagation effects are included in the path loss [6]. It is presented in the value of  $\bar{E} = 30 \text{ dB } \mu\text{V/m}$  in this paper (Fig. 10).



#### 4 Comparison of Theoretical and Experimental Results

The ray that undergoes lesser interaction with objects in Site A before it intersects with the receiving antenna or that takes the shortest path from the transmitting antenna to the receiving antenna is assumed to be the main contribution to the received signal. This assumption is made because increased interactions produce increased losses, so the ray with the fewest interactions will have the smallest losses. Therefore, the ray with the fewest interactions contributes to a higher signal level than any of the other rays that have more extensive interactions with obstacles. In this work, we designated the ray with the fewest interactions as single ray 1. Single ray 2 also was identified through the image concept, but it does not obey the condition mentioned above. The combination of single ray 1 and single ray 2 is designated as “2 ray,” which is closer to reality, since the receiving antenna does not receive just a single ray. The 2 ray model is developed based on the two shortest path that taken by the received ray (wave signal) in a particular measuring position. Therefore, it is volatile for each measuring position in all measurement sites.

The normalized path loss is the ratio of the power of the received signal at a particular distance to the received signal at the reference distance (1 m) in Site A as mentioned in section C, namely the far field that considers only the radiating field.

The absolute mean error and shown in Table 1 indicate the effectiveness of each method in predicting the strength of the received signal or the path loss. Meanwhile, the errors that are shown in Tables 1, 2, 3, 4 were obtained from the differences between measured data at

**Table 1** Site A

Method	Position (P)	Error (dB)	Absolute mean error (dB)
Single ray 1	P1	-1.57	1.61
	P2	-3.51	
	P3	1.42	
	P4	-0.32	
	P5	1.22	
Single ray 2	P1	-11.2	15.85
	P2	21.67	
	P3	-24.48	
	P4	14.78	
	P5	-7.12	
2 rays	P1	-1.06	8.07
	P2	21.36	
	P3	1.85	
	P4	13.12	
	P5	2.94	
Direct ray	P1	4.24	11.91
	P2	12.48	
	P3	13.04	
	P4	17.92	
	P5	11.85	

**Table 2** Site B

Method	Position (P)	Error (dB)	Absolute mean error (dB)
Single ray 1	P1	2.41	2.31
	P2	-4.02	
	P3	-4.84	
	P4	0.26	
	P5	0.01	
Single ray 2	P1	-36.38	20.62
	P2	12.24	
	P3	-37.83	
	P4	2.44	
	P5	-14.22	
2 rays	P1	2.31	4.28
	P2	12.02	
	P3	-4.76	
	P4	1.57	
	P5	0.74	
Direct ray	P1	1.63	6.74
	P2	15.71	
	P3	-1.33	
	P4	11.76	
	P5	4.18	

specific positions and the theoretical results provided by Eqs. (1) and (2). These equations are used to find reflection coefficient, transmission coefficient, and diffraction coefficient. The receiving ray at each position takes a different path or encounters a different mechanism before reaching the receiving antenna. The huge absolute mean error in single ray 2 (15.85 dB) implied that it cannot be implemented independently. Therefore, to improve the accuracy, it should be only the 'supplement' to single ray 1. Unfortunately, single ray 2 fails to achieve that, causing the 2 ray to be maintained at an absolute mean error level of 8.07 dB, which is significantly greater than the absolute mean error level of the single ray 1, i.e., 1.61 dB. The phase angle plays a very important role, and in this case, the association between single ray 1 and single ray 2 with its phase angle to form the 2 ray was insufficient to provide accurate results.

The direct ray also has a high absolute mean error (11.91 dB) compared to the single ray 1, as shown in Table 1. Distance factor is not the main reason that causes the loss in Site A, but obstruction losses are the dominant factor in the loss of field strength.

The characteristics or features of Site B are similar to those of Site A. A comparison of Figs. 11 and 12 indicates that the path losses due to the free space assumption were similar for Site A and Site B. Considering distance, there is not much attenuation due to the free space loss.

The absolute mean errors of each method listed in Table 2 do not show any deviant cases. The absolute mean error for single ray 2 was the largest (20.62 dB) among the rest of the methods, while single ray 1 had the lowest absolute mean error of just 2.31 dB. Single ray

**Table 3** Site C

Method	Position (P)	Error (dB)	Absolute mean error (dB)
Single ray 1	P1	1.94	3.07
	P2	2.25	
	P3	0.35	
	P4	7.32	
	P5	3.50	
Single ray 2	P1	-20.55	8.78
	P2	-5.63	
	P3	-5.80	
	P4	7.13	
	P5	4.80	
2 rays	P1	2.41	3.74
	P2	3.39	
	P3	1.20	
	P4	11.62	
	P5	-0.06	
Direct ray	P1	4.16	5.46
	P2	7.23	
	P3	2.77	
	P4	8.72	
	P5	5.91	

2, 2 ray, and direct ray underwent the same problems as mentioned for Site A. However, the absolute mean error of 2 ray (4.28 dB) and direct ray (6.74 dB) (Table 2) for Site B were in slight agreement when the measured data for the 2 ray (8.07 dB) and the direct ray (11.91 dB) in Site A were compared (Table 1). The sum of two rays that will be obtained by involving the phase angle is very difficult to predict.

The ray-tracing technique must be fully implemented in the positions in Site C to trace possible ray path. The ray-tracing technique may trace more than one ray path. However, one of the rays is the main contributor (single ray 1), and the other can be considered as “supplement” ray (single ray 2) to raise its accuracy. All of the performance conditions are illustrated in Fig. 12.

As shown in Table 3, the performance of single ray 1 was as expected, giving a relatively small absolute mean error between the measured and the predicted path loss, i.e., 3.07 dB. However, the performance of the 2 ray model (absolute mean error of 3.74 dB) was not what we expected, i.e., the model was expected to obtain better than the model for single ray 1. The 2 ray model was a combination of the single ray 1 and single ray 2 models, and it can be defined as a contributor that improved by single ray 2. The absolute mean error of the 2 ray model seemed greater than that of the single ray 1. This observation indicates that, to improve the accuracy, the phases of both single ray models in their modes of superposition (either constructively or destructively) must be accounted for, because they determine the effectiveness of the 2 ray model. The truncation of three or more rays that are only constituted of single ray 1 and single ray 2 in the 2 ray may affect the accuracy of its predictions.

**Table 4** Site D

Method	Position (P)	Error (dB)	Absolute mean error (dB)
Single ray 1	P1	5.05	2.84
	P2	2.26	
	P3	-1.28	
	P4	-2.57	
	P5	2.45	
	P6	-3.44	
Single ray 2	P1	-8.66	15.45
	P2	-33.61	
	P3	-15.56	
	P4	-14.28	
	P5	-13.94	
	P6	-6.63	
2 rays	P1	3.91	2.22
	P2	2.12	
	P3	-2.37	
	P4	-3.19	
	P5	0.63	
	P6	1.09	
Direct ray	P1	7.75	12.22
	P2	7.00	
	P3	11.81	
	P4	18.82	
	P5	11.59	
	P6	18.16	

The results from the direct ray provide a reference for comparison to the other models to pinpoint the loss. The subtraction of the loss is due to the small-scale fading, such as the multi-path effect, and to large-scale fading caused by obstruction losses.

The influence of the concrete pillars and the glass windows in Site C cannot be ignored, since some additional rays or overweighed rays will be received and may cause an inaccurate prediction [8], which is made evident by the large absolute mean error of the direct ray condition listed in Table 4. Therefore, the ray-tracing process must be conducted to prevent large discrepancies between the theoretical and measured results.

The results of the single ray and 2 ray models were in good agreement with the measured data, as indicated by the absolute mean errors of 2.84 and 2.22 dB (Table 4) compared to the single ray 2 and the direct ray methods. The multipath interference in Site C was not as severe as it was in Site D, where there were more people and greater human activity [9]. This is readily apparent when the absolute mean errors shown in Tables 3 and 4 are compared.

Since Site D is located in the NLOS region, the direct ray condition with the assumption of free space propagation cannot be made. It can be proved by Table 4 or Fig. 13, in which the absolute mean error is shown to be greater than those for single ray 1 and 2 ray in Table 4.

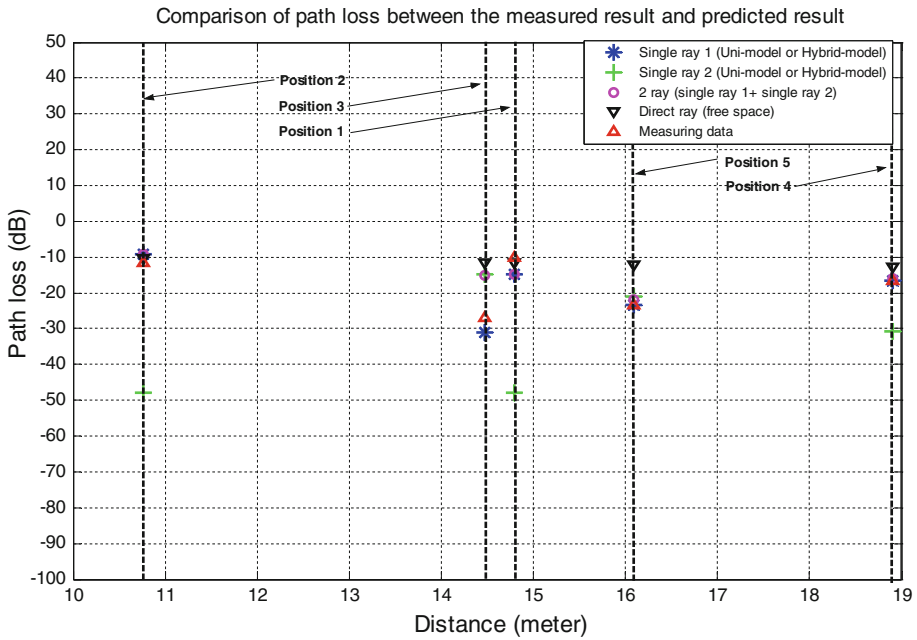


Fig. 11 Statistical comparison between the measured path loss and the predicted path loss for Site B

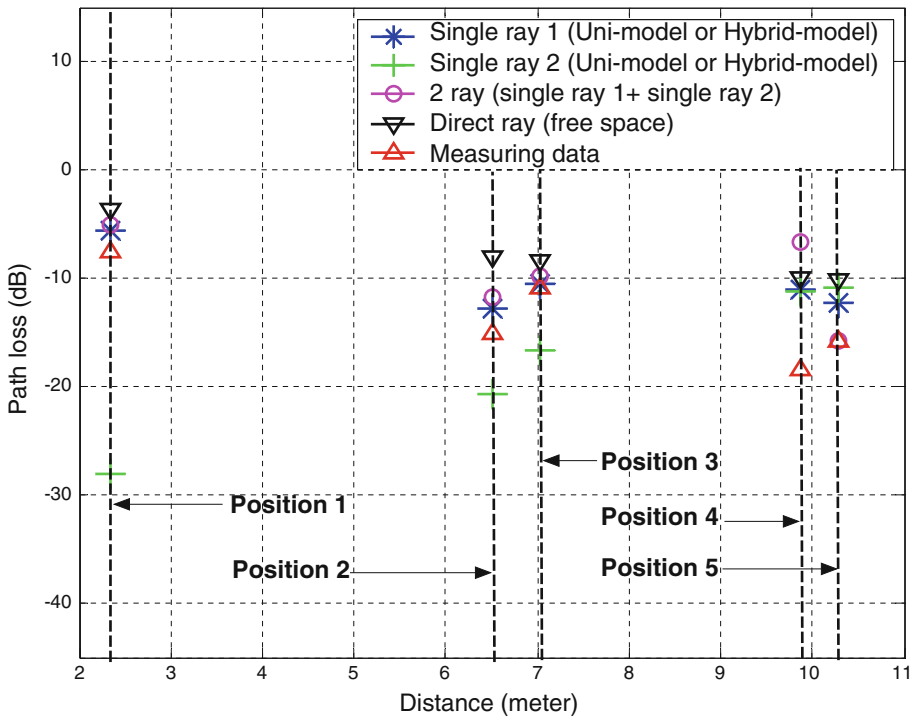
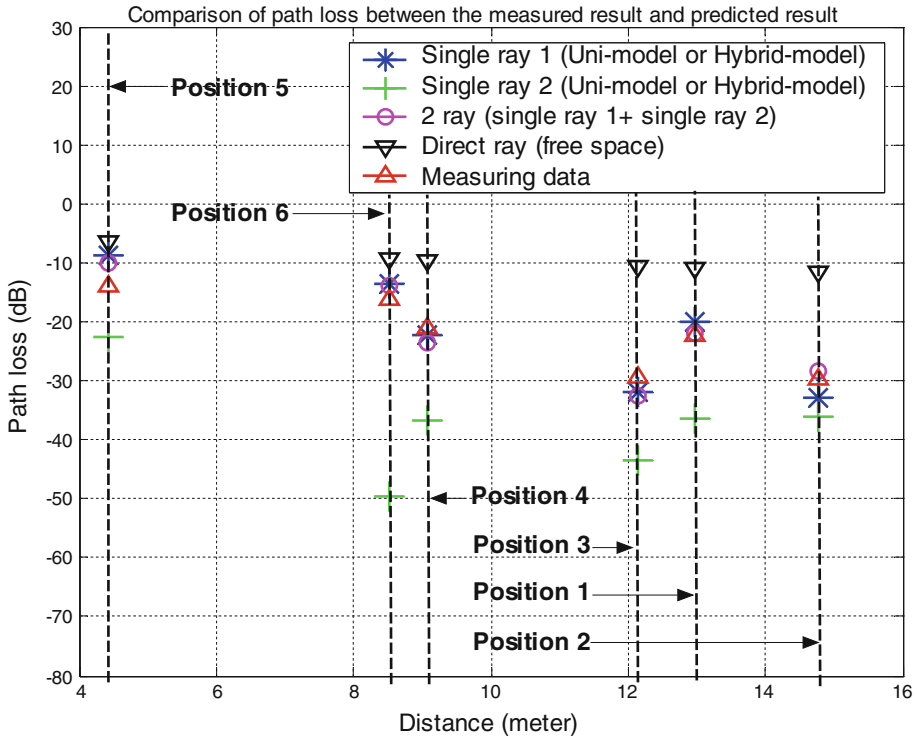


Fig. 12 Comparison between the measured results and the predicted results for Site C



**Fig. 13** Statistical comparison of the measured path loss and the predicted path loss for Site D

The case of single ray 2 in Site D was also similar in Sites A, B, and C in which the single ray 2 acts as a ‘supplement’ to the single ray 1 to improve the accuracy.

Theoretically, the temporal variation of signal strength in Site D was severe because Site D is an office, and there were people moving around. Temporal variation of signal strength is subject to either mobile obstacles or furniture (e.g., chairs, files, and computers) in the office (Site D). Systems must be designed with enough signal margins to accommodate these fluctuations. Furthermore, these effects are unavoidable while collecting data in real-world situations, so they were ignored in this study [7].

### 5 Conclusions

In this project, a path loss model for indoor environments is developed using geometrical optics (GO) and uniform theory of diffraction (UTD). The study involved making comparisons of the measured and predicted path loss values at various positions in the Division of Information Technology at Universiti Putra Malaysia. Supposedly, the direct ray model is used for prediction in the Line-Of-Sight (LOS) region. However, this work was associated with the reflection coefficient, transmission coefficient, and diffraction coefficient, thereby forming a new model for predicting the loss of signal strength in an NLOS signal path. For the NLOS region in the Division of Information Technology, most of the single ray 1, which

was the main contributor to the strength of the received signal, showed good agreement with the measured path losses, with an absolute mean error less than 3.5 dB for all measurements.

Infinite rays can be considered by implementing simulations of the “brute-force” ray-tracing technique. However, this technique requires high performance computing equipment to simulate the concepts of infinite rays.

**Acknowledgments** The author thanks the staff members in the Division Information Technology, University Putra Malaysia, for their assistance in setting up and conducting the measurements described here.

## References

1. Nešković, A., Nešković, N., & Paunović, D. (2000). Modern approaches in modeling of mobile radio systems propagation environment. In *IEEE communications surveys, third quarter* (pp. 2–12).
2. Ernst, B. In *Digital mobile radio towards future generation systems: cost 231 final report: Tunnel, corridors, and other special environments* (pp. 190–207). Austria: Technical University of Vienna.
3. Balanis, C. A. (1989). *Advanced engineering electromagnetics*. Canada: John Wiley & Sons Inc.
4. McNamara, D. A., Pistorius, C. W. I., & Malherbe, J. A. G. (1990). *Introduction to the uniform geometrical theory of diffraction*. Boston: Artech House.
5. Remley, K. A., Anderson, H. R., & Weissnar, A. (2000). Improving the accuracy of ray-tracing techniques for indoor propagation modeling. *IEEE Transactions on Vehicular Technology*, 49(6), 2350–2358.
6. Kwok-Wai Cheung Sau, J. H.-M., & Murch, R. D. (1998). A new empirical model for indoor propagation prediction. *IEEE Transactions on Vehicular Technology*, 47(3), 996–1001.
7. Valenzuela, R. A., Landron, O., & Jacobs, D. L. (1997). Estimating local mean signal strength of indoor multipath propagation. *IEEE Transactions on Vehicular Technology*, 46(1), 203–212.
8. Collonge, S., Zaharia, G., & El Zein, G. (2004). Influence of human activity on wide-band characteristics of the 60 GHz indoor radio channel. *IEEE Transactions on Wireless Communication*, 3(6), 2396–2406.
9. Tarnag, J. H., & Liu, T. R. (1999). Effective models in evaluating radio coverage on single floors of multi-floor buildings. *IEEE Transactions on Vehicular Technology*, 48(3), 203–212.

## Author Biographies



**E. M. Cheng** was born in 1980. He obtained his B.Sc. (Honours)-Instrumentation Science in Universiti Putra Malaysia in 2004. He pursued his M.Sc. in Wave Propagation at the Institute for Mathematical Research on 2005 in Universiti Putra Malaysia and his Ph.D. in Microwave at the Faculty of Science in 2007 in Universiti Putra Malaysia. Recently, he is a senior lecturer in School of Mechatronic Engineering, Universiti Malaysia Perlis. His main personnel research interest is in the computational electromagnetic modeling, microwave dielectric spectroscopy and microwave sensors development for agricultural applications.



**Zulkify Abbas** was born in Alor Setar, Malaysia, in 1962. He received the B.Sc. degree with honors in physics from the University of Malaysia, Kuala Lumpur, in 1986, the M.Sc. degree in microwave instrumentation from the Universiti Putra Malaysia (UPM), Serdang, in 1994, and the Ph.D. degree in electronic and electrical engineering from the University of Leeds, Leeds, U.K., in 2000. He is currently a Associate Professor with the Department of Physics, UPM, where he has been a faculty member since 1987. His main personnel research interest is in the theory, simulation, and instrumentation of electromagnetic wave propagation at microwave frequencies focusing on the development of microwave sensors for agricultural applications.



**M. Fareq** obtained his B.E. (Honours)- Electronic and Communication Engineering in The University of Birmingham, United Kingdom in 1994. He pursued his M.Sc. (Eng) in Microelectronic Systems and Telecommunications at the The University of Liverpool, United Kingdom on 2003 and Ph.D. Electrical Engineering (Radio Frequency and Microwave) on 2005 in The University of Liverpool, United Kingdom. Recently, he is Dean in School of Electrical System Engineering, Universiti Malaysia Perlis. His main personnel research interest is in the computational electromagnetic modeling, antenna system design and microwave absorber fabrication etc.

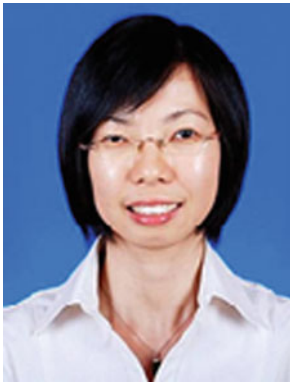


**K. Y. Lee** was born in Muar, Johor, Malaysia. He received his B.Sc. Physics, M.Sc. Microwaves, and Ph.D. Microwaves all from the Universiti Putra Malaysia in year 2002, 2004, and 2008 respectively. In December 2007, He joined Universiti Tunku Abdul Rahman as a Lecturer in Department of Electronics and Electrical Engineering. His areas of research include microwave measurement technique, microwave circuit and instrumentation, control and automation, material properties measurement, and instrumentation calibration.





**K. Y. You** was born in 1977. He obtained his B.Sc. Physics (Honours) degree in Universiti Kebangsaan Malaysia in 2001. He pursued his M.Sc. in Microwave at the Faculty of Science in 2003 and his Ph.D. in Wave Propagation at the Institute for Mathematical Research in 2006 in Universiti Putra Malaysia. Recently, he is a senior lecturer at Radio Communication Engineering Department, Universiti Teknologi Malaysia. His main personnel research interest is in the theory, simulation, and instrumentation of electromagnetic wave propagation at microwave frequencies focusing on the development of microwave sensors for agricultural applications.



**S. F. Khor** was born in 1982. She obtained her B.Sc. with Edu. (Honours)-Physics in Universiti Putra Malaysia in 2007. She pursued her Ph.D. in Materials Science at the Faculty of Science in 2011 in Universiti Putra Malaysia. Recently, she is a senior lecturer at School of Electrical Systems Engineering, Universiti Malaysia Perlis (UniMAP). Her main personnel research interest is in the glass science and focusing on dielectric, optical, mechanical and thermal properties.